Electronic Supplementary Material (ESI) for Materials Chemistry Frontiers.

Facile preparation of fluorescent non-conjugated polymer films with tunable multicolor photoluminescence by layer-by-layer assembly

Xu Wang[a], Huyun Sun[a], Yingxi Lu[a,*], and Xianfeng Zhou[b,*]

[a] College of Materials Science and Engineering, Qingdao University of Science and Technology, Qingdao 266042, P. R. China

[b] College of Polymer Science and Engineering, Qingdao University of Science and Technology, Qingdao 266042, P. R. China

1. Experiments and Equipments

1.1 Materials

Branched polyethylenimine (PEI, Mn ~60,000) was purchased from Acros Organics. Poly(acrylic acid) (PAA, Mw ~450,000) and zinc sulfate heptahydrate were purchased form Aldrich. Iron trichloride hexahydrate and calcium chloride anhydrous were purchased from Sinopharm Chemical Reagent Co., Ltd. Nickel chloride hexahydrate, magnesium chloride hexahydrate and manganese chloride tetrahydrate were purchased from Macklin. Barium chloride dehydrate was purchased from Tianjin Beilian Fine Chemicals Development Co., Ltd. Aluminum sulfate was purchased from Tianjin Zhiyuan Chemical Reagent Co. Ltd. Sodium chloride and potassium chloride were purchased from Genaral-Reagent and TCL, respectively. All chemicals were used without further purification. Deionized water (DI, pH ~6.5) was used for all the experiments.

1.2 Preparation of layer-by-layer assembled polymeric films

The newly cleaned quartz slide was immersed in PEI aqueous solution for ~20 min to obtain a PEI-modified surface and was ready for the multilayers deposition. The LbL deposition of PAA/PEI multilayer films was conducted automatically by a programmable dipping machine (SYDC-100 M, Shanghai SAN-YAN Technology Co., Ltd) at room temperature. The PEI-

modified substrate was immersed in 4 mg/mL PAA (pH adjusted to 2.5 with 1 M NaOH and 1 M HCl) for 15 min to obtain a layer of PAA polymer. The substrate was then immersed in DI water for 1 min two times. Next, the substrate was immersed in aqueous solution of 4 mg/mL PEI (pH adjusted to 8.5) for 15 min to obtain a layer of PEI polymer, followed by immersing in DI water for 1 min two times. Repetition of the above procedure allows the preparation of multilayer films of PAA/PEI, as shown in Scheme 1. Similar assembling processes by LbL assembly were described in the literatures.[1, 2] All the substrates were not dried between the adsorption steps but were blown dry with N_2 gas after the final step of the film deposition. All the assembled (PAA/PEI)*n multilayer films were heated at 50 ℃ for 1 h in an oven to remove the physically absorbed water in the polymeric films.

All samples for Fourier transform infrared (FTIR) measurements were prepared on the CaF_2 substrates. Before assembling, the plasma treatment was produced to obtain a reactive hydrophilic surface on the CaF_2 substrates. Then pure PEI monolayer and (PAA/PEI)*5 multilayers were assembled by the same LbL-deposition method. The sample of pure PAA was prepared by drop-casting method.

1.3 Sample characterizations

UV-vis spectra were recorded using a HITACHI U-2910 spectrophotometer. Fluorescence microscopic images for the LbL-assembled polymeric films were recorded using an inverted fluorescence microscope of OLYMPUS IX73. Nanosecond fluorescence lifetime experiments were performed by the time-correlated single-photon counting (TCSPC) system. A 375 nm picosecond diode laser (Edinburgh Instruments EPL-375) was used to excite the samples. The fluorescence was collected by a photomultiplier tube that was connected to a TCSPC board (Edinburgh Instruments FLS-1000). FTIR spectroscopy was performed on a JASCO-FT/IR-4700 in a transmission mode at a scan resolution of 4 cm^{-1}.

1.4 Fluorescence quenching effect by metal ions

The fluorescence excitation/emission spectra and quantum yield were recorded on a FS5 fluorescence spectrometer (Edinburgh Instruments) at room temperature. The fluorescence quenching experiments were performed by immersing the (PAA/PEI)*n multilayer films in aqueous solution of various metal ions for a period of time and then collecting the fluorescence data at the excitation wavelength of 340 nm, immediately. All of the fluorescence detections were under the same conditions: the excitation and emission silt width were set at 2 nm and 5 nm, respectively. Nanosecond fluorescence lifetime experiments were performed on a FLS-1000 Fluorescence Spectrometer (Edinburgh Instruments).

2. Supporting Data

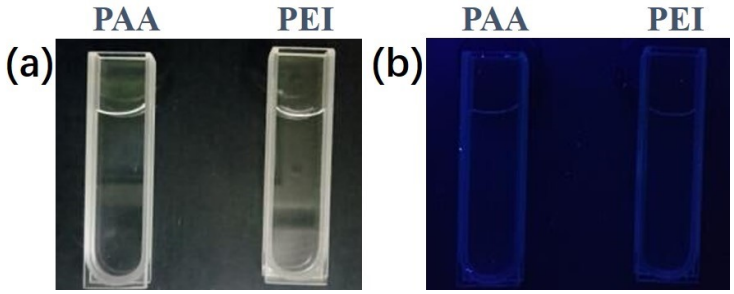

Figure S1. Digital photographs of 4 mg/mL PAA and 4 mg/mL PEI solutions under the visible light (a) and UV light of 365 nm (b).

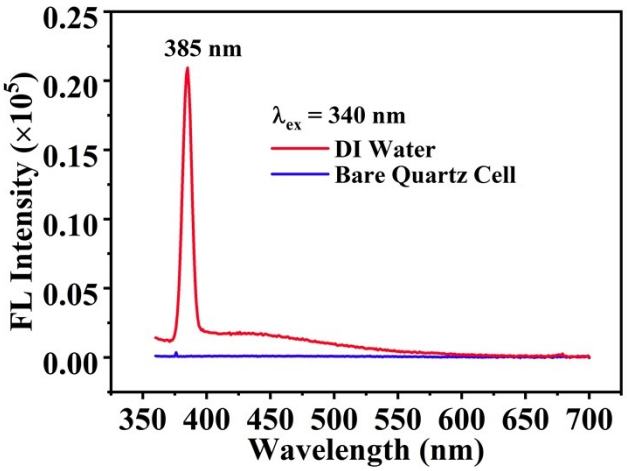

Figure S2. Fluorescence spectra of bare quartz cell and DI water excited at 340 nm.

In reality, the peak at 385 nm is the Raman scattering peak of water when excited at 340 nm, which is superimposed atop the fluorescence emission.

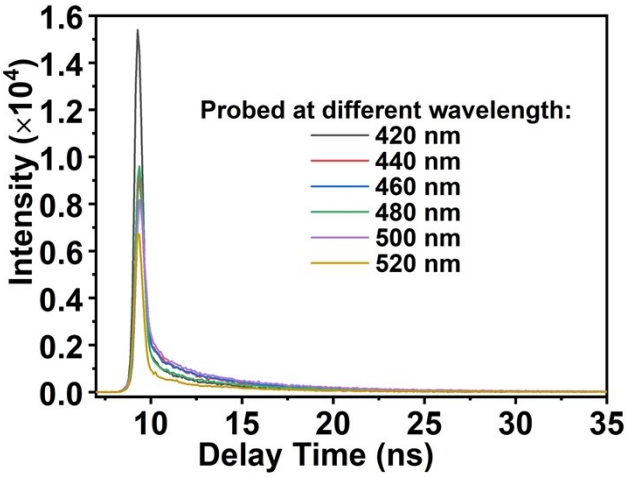

Figure S3. PL lifetime of the (PAA/PEI)*100 multilayers at 375 nm excitation and probed from 420 to 520 nm.

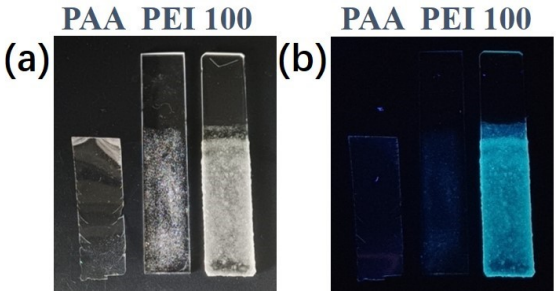

Figure S4. Digital photographs of dry PAA film (left), PEI film (middle) and (PAA/PEI)*100 multilayers (right) under the visible light (a) and UV light of 365 nm (b).

Pristine PAA powders were dissolved with a little DI water and then put in a vacuum oven at 50 °C for 2 days. A dry film of PAA was then obtained (left sample). Pristine PEI solution (50 wt.%) couldn't be dried by this way even after drying for one week. Therefore, freeze drier was

used. After freezing for up to one week, a viscous PEI solution was obtained, but not a dry PEI film. Then the viscous PEI solution was coated on a quartz slide (middle sample).

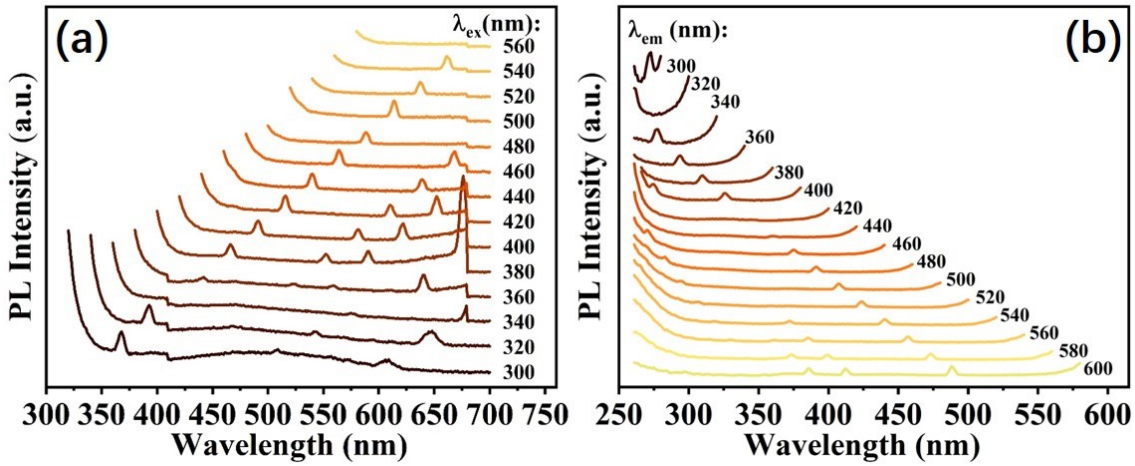

Figure S5. (a) Emission and (b) excitation spectra of the bare quartz slide when excited and emitted at different wavelength, respectively.

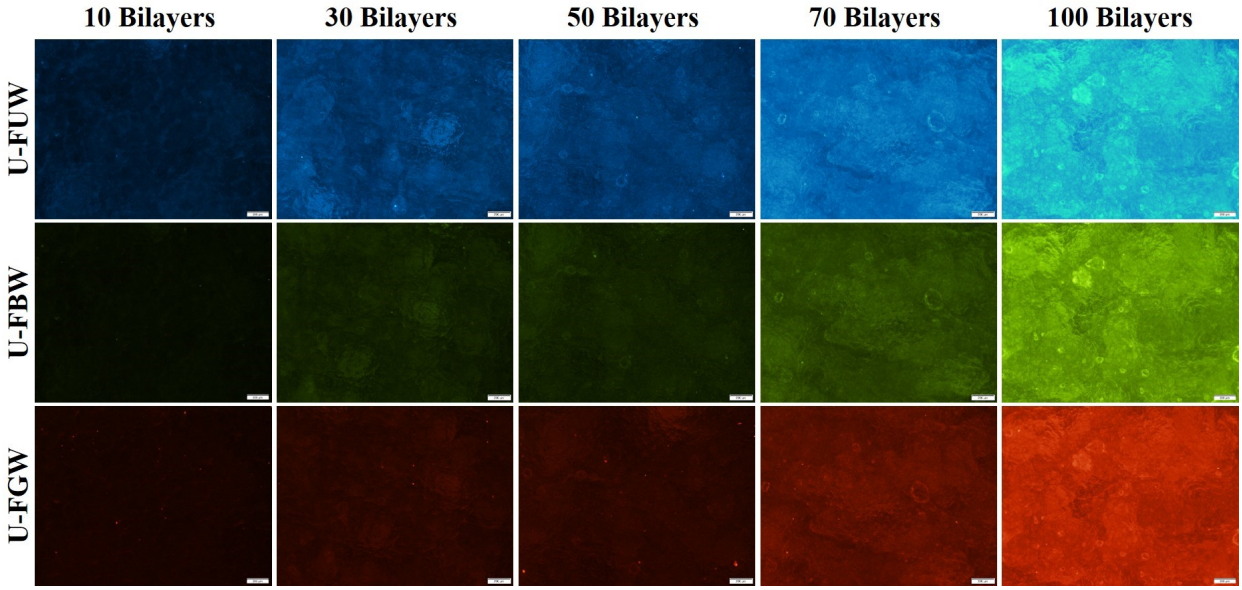

Figure S6. Fluorescence microcopy images of (PAA/PEI)*n multilayers membranes excited by UV, blue, and green lights using three mirror units of U-FUW (exciter filter 340-390 nm), U-

FBW (exciter filter 460-495 nm), and U-FGW (exciter filter 530-550 nm), respectively. The scale bar is 200 μm. The exposure time is fixed at 210.5 ms for U-FUW unit, 526.3 ms for U-FBW unit, 2.4 s for U-FGW unit, respectively.

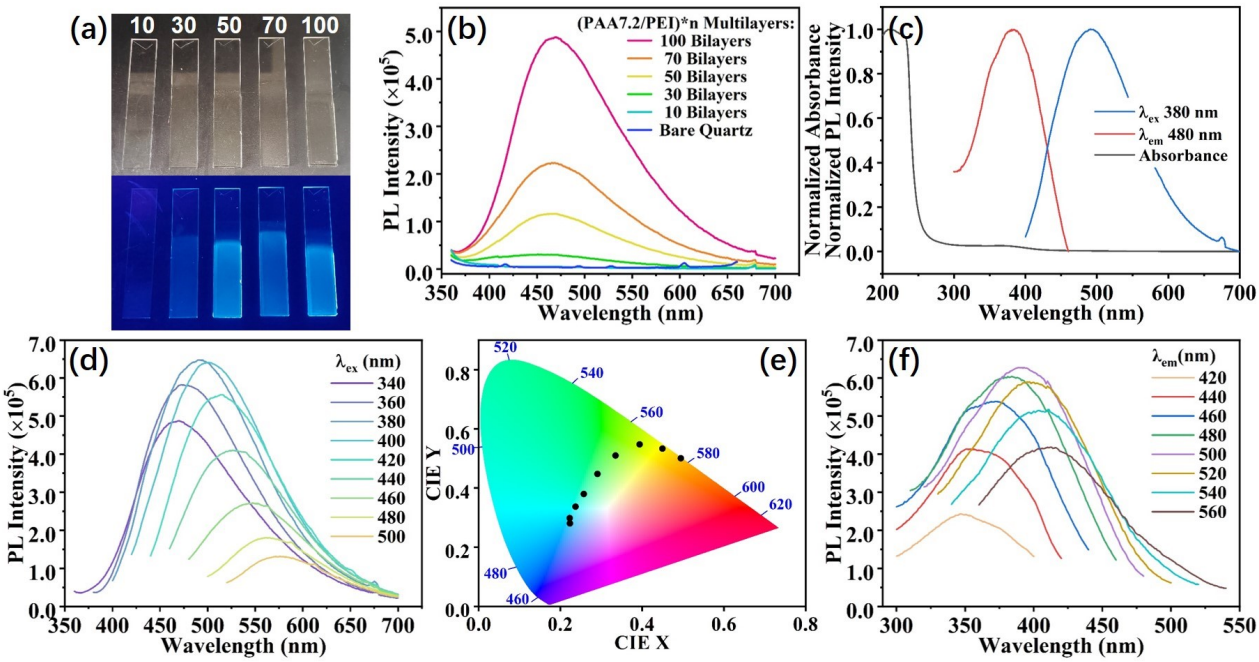

Figure S7. Fluorescence characteristics of (PAA7.2/PEI)*n polymeric multilayers. (a) Photographs of (PAA7.2/PEI)*n multilayers with different bilayers under the visible light (top) and UV light of 365 nm (down). (b) Fluorescence spectra of the (PAA7.2/PEI)*n multilayers with different bilayers excited at 340 nm. (c) Normalized absorbance and fluorescence spectra, (d) emission spectra, (e) commission internationale de l'Eclairage (1931) coordinates and (f) excitation spectra, respectively.

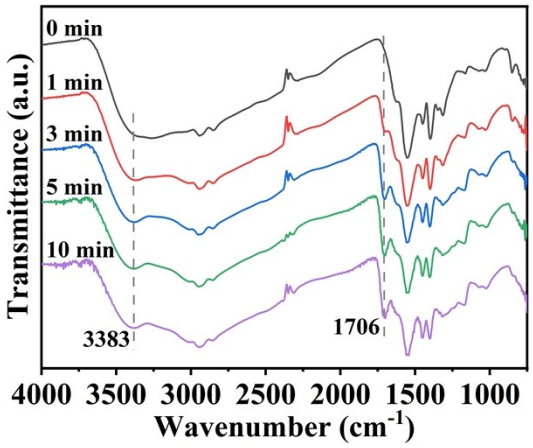

Figure S8. FTIR spectra of (PAA/PEI)*5 multilayers upon immersing in 3.0 mM Fe^{3+} solution with different time.

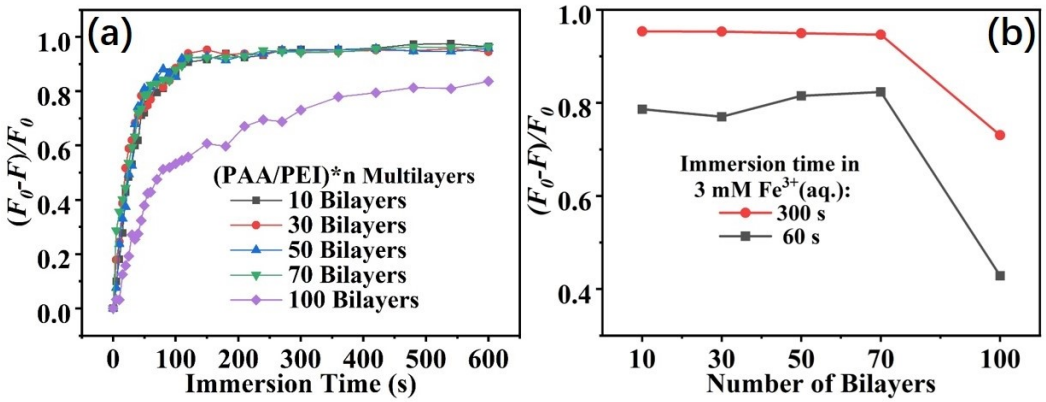

Figure S9. Changes in $(F_0-F)/F_0$ (λ = 405 nm) of (PAA/PEI)*n multilayers with different bilayers upon the different immersion time in 3.0 mM Fe^{3+} solution.

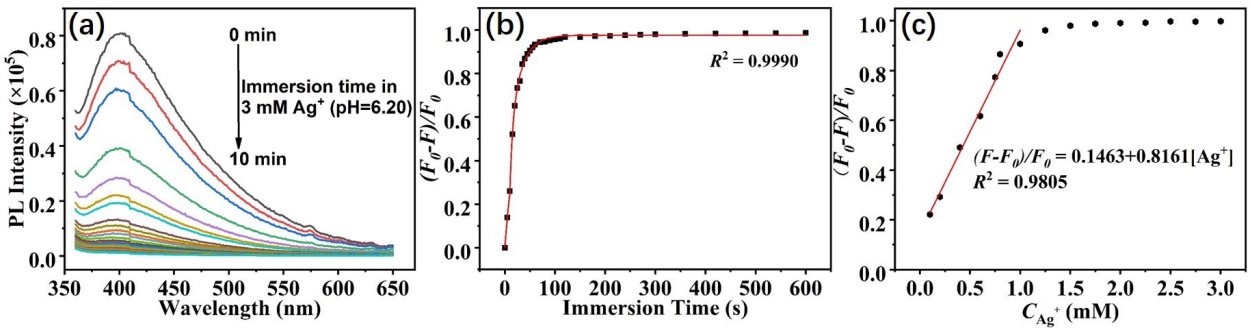

Figure S10. Changes in the emission spectra (λ_{ex} = 340 nm) (a) and the fluorescence quenching ratio (b) of (PAA/PEI)*30 multilayers upon the different immersion time in 3.0 mM Ag^+ ions. (c) Relationship between $(F_0\text{-}F)/F_0$ and different concentrations of Ag^+ ions.

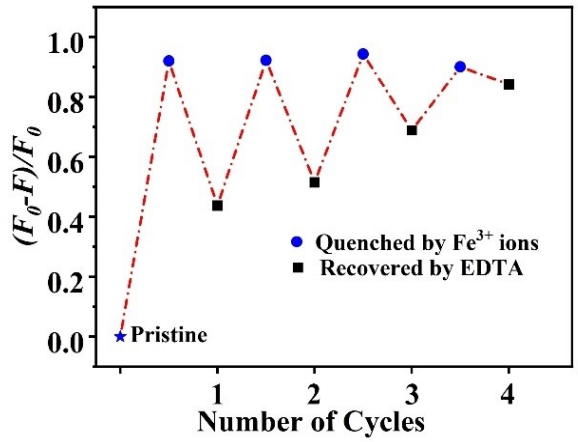

Figure S11. Quenching and recovery tests of (PAA/PEI)*30 multilayers for Fe^{3+}. The used concentrations are 3 mM Fe^{3+} and 5 mM EDTA, respectively.

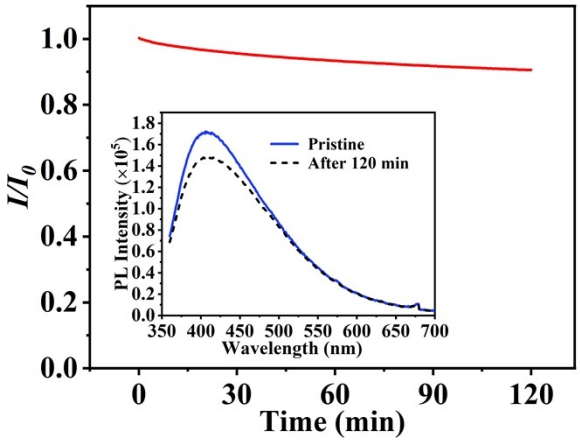

Fig S12. Photofading behavior of the (PAA/PEI)*30 multilayers (λ_{ex}=340 nm). The experiment was conducted with Edinburgh FS5 fluorescence spectrophotometer, which is equipped with 150-Watts CW Ozone-free Xenon arc lamp. The inset is the change in fluorescence emission spectra of (PAA/PEI)*30 multilayers before and after light irradiation.

Table S1. Lifetime of the (PAA/PEI)*100 multilayers at 375 nm excitation and probed at different wavelength sections.

Wavelength (nm)	**τ_1 (ns)**	**Percent (%)**	**τ_2 (ns)**	**Percent (%)**	**τ_3 (ns)**	**Percent (%)**	**$\tau_{averange}$ (ns)**	**χ^2**
440	0.24	24.95	2.77	46.54	7.76	28.52	3.56219	1.301
460	0.25	25.31	3.25	45.96	8.51	28.72	4.001047	1.294
480	0.22	34.21	2.96	32.95	7.79	32.85	3.609597	1.448
500	0.28	22.61	3.01	39.27	8.28	38.12	4.401671	1.301
520	0.24	41.74	2.44	23.68	7.2	34.58	3.167728	1.346

Table S2. Comparison of sensing performance of different fluorescent probes for Fe^{3+} ions detection.

Type of probe	Preparation Methods	Linear Range (mM)	LOD (mM)	Solvents	Ref.
Polyurethane foam based on rhodamine derivative	Synthesis	0.02-0.1	1.64×10^{-3}	water	[3]
Poly(5-cyanoindole) film	Electro-polymerization	2.0×10^{-4}-0.5	1.6×10^{-5}	water	[4]
Poly(1-amino-5-chloroanthraquinone)	Polymerization.	1.0×10^{-7}-0.1	2.0×10^{-8}	DMF/H_2O	[5]
Probes based on rhodamine B/amino acid derivatives (RhB-His)	Step-synthesis	0-0.02	2.5×10^{-4}	EtOH/ PBS buffer	[6]
Conjugated microporous organic polymer (TPA-Bp)	Schiff-base reaction	0-0.2	1.02×10^{-2}	DMF	[7]
Conjugated polymer combined with rhodamine spirolactam (CP1)	Synthesis	0-0.1	3.0×10^{-4}	Tris-HCl buffer	[8]
Nile red functionalized graphene film (po-Gr-Nr)	Electrochemical exfoliation	0.03-1.0	2.49×10^{-2}	water	[9]
Nitrogen-doped carbon quantum dots with chitosan (N-CQDs)	Hydrothermal method	0-0.2	1.5×10^{-4}	water	[10]
“Vigna radiata” based C-dots	Hydrothermal carbonization	0.1-2	1.4×10^{-4}	water	[11]
Chitin based C-dots	Synthesis (deep eutectic solvent treatment)	0.04-0.6	4.3×10^{-4}	water	[12]
S. chinensis polysaccharide based C-dots	Ethanol precipitation and hydrothermal carbonization	0.1-1	5.7×10^{-4}	water	[13]
Tetraphenylethylene-based covalent organic framework (TTPE-COF)	Schiff-base reaction	0.01-10	3.07×10^{-3}	water	[14]
Terbium(III) lanthanide–organic framework (534-MOF-Tb)	Solvothermal reaction	0-0.1	0.13	water	[15]
$[(CH_3)_2NH_2]\cdot[Tb(bptc)]\cdot$ xsolvents (MOF)	Solvothermal reaction	0-0.1	0.1801	EtOH	[16]
Eu^{3+}@UiO-66(20)-based MOF	Hydrothermal reaction	0-1.2	1.28×10^{-2}	water	[17]
(PAA/PEI)*30 films	LbL assembly	0.1-3.0	7.6×10^{-2}	water	This work

References:

[1] X. Wang, R. Wang, F. Wu, H. Yue, Z. Cui, X. Zhou, Y. Lu, Mussel-inspired layer-by-layer assembled polymeric films with fast growing and NIR light triggered healing capabilities, Eur. Polym. J. 158 (2021) 110689.

[2] D. Chen, M. Wu, B. Li, K. Ren, Z. Cheng, J. Ji, Y. Li, J. Sun, Layer-by-layer assembled healable antifouling films, Adv. Mater. 27 (2015) 5882–5888.

[3] Y. Chen, Y. Wu, Y. Zhu, S. Tian, A fluorescent polyurethane foam based on rhodamine derivative as Fe(III) sensor in pure water, Polym. Int. 71 (2021) 169–174.
[4] W. Ding, J. Xu, Y. Wen, H. Zhang, J. Zhang, Facile fabrication of fluorescent poly(5-cyanoindole) thin film sensor via electropolymerization for detection of Fe^{3+} in aqueous solution, Journal of Photochemistry and Photobiology A: Chemistry 314 (2016) 22–28.
[5] S. Huang, P. Du, C. Min, Y. Liao, H. Sun, Y. Jiang, Poly(1-amino-5-chloroanthraquinone): Highly selective and ultrasensitive fluorescent chemosensor for ferric ion, J Fluoresc 23 (2013) 621–627.
[6] H. Li, Z. Liu, R. Jia, "Turn-on" fluorescent probes based on Rhodamine B/amino acid derivatives for detection of Fe^{3+} in water, Spectrochim Acta A Mol Biomol Spectrosc 247 (2021) 119095.
[7] C. Zhang, G. Pan, Y. He, Conjugated microporous organic polymer as fluorescent chemosensor for detection of Fe^{3+} and Fe^{2+} ions with high selectivity and sensitivity, Talanta 236 (2022) 122872.
[8] Y.X. Wu, J.B. Li, L.H. Liang, D.Q. Lu, J. Zhang, G.J. Mao, L.Y. Zhou, X.B. Zhang, W. Tan, G.L. Shen, R.Q. Yu, A rhodamine-appended water-soluble conjugated polymer: An efficient ratiometric fluorescence sensing platform for intracellular metal-ion probing, Chem Commun (Camb) 50 (2014) 2040–2042.
[9] O. Sadak, A.K. Sundramoorthy, S. Gunasekaran, Highly selective colorimetric and electrochemical sensing of iron (III) using Nile red functionalized graphene film, Biosensors and Bioelectronics 89 (2017) 430–436.
[10] L. Zhao, Y. Wang, X. Zhao, Y. Deng, Y. Xia, Facile synthesis of nitrogen-doped carbon quantum dots with chitosan for fluorescent detection of Fe^{3+}, Polymers (Basel) 11 (2019) 1731.
[11] N. Kaur, V. Sharma, P. Tiwari, A.K. Saini, S.M. Mobin, "Vigna radiata" based green C-dots: Photo-triggered theranostics, fluorescent sensor for extracellular and intracellular iron (III) and multicolor live cell imaging probe, Sensors and Actuators B: Chemical 291 (2019) 275–286.
[12] M. Feng, Y. Wang, B. He, X. Chen, J. Sun, Chitin-based carbon dots with tunable photoluminescence for Fe^{3+} detection, ACS Applied Nano Materials 5 (2022) 7502–7511.
[13] X. Wu, C. Ma, J. Liu, Y. Liu, S. Luo, M. Xu, P. Wu, W. Li, S. Liu, In situ green synthesis of nitrogen-doped carbon-dot-based room-temperature phosphorescent materials for visual iron ion detection, ACS Sustainable Chemistry & Engineering 7 (2019) 18801–18809.
[14] D. Cui, X. Ding, W. Xie, G. Xu, Z. Su, Y. Xu, Y. Xie, A tetraphenylethylene-based covalent organic framework for waste gas adsorption and highly selective detection of Fe^{3+}, CrystEngComm 23 (2021) 5569–5574.
[15] M. Chen, W.-M. Xu, J.-Y. Tian, H. Cui, J.-X. Zhang, C.-S. Liu, M. Du, A terbium(iii) lanthanide–organic framework as a platform for a recyclable multi-responsive luminescent sensor, Journal of Materials Chemistry C 5 (2017) 2015–2021.
[16] X.-L. Zhao, D. Tian, Q. Gao, H.-W. Sun, J. Xu, X.-H. Bu, A chiral lanthanide metal–organic framework for selective sensing of Fe(iii) ions, Dalton Transactions 45 (2016) 1040–1046.
[17] L. Li, S. Shen, W. Ai, S. Song, Y. Bai, H. Liu, Facilely synthesized Eu^{3+} post-functionalized UiO-66-type metal-organic framework for rapid and highly selective detection of Fe^{3+} in aqueous solution, Sens. Actuators, B 267 (2018) 542–548.